JCTC Journal of Chemical Theory and Computation

Geometry Optimization of Large and Flexible van der Waals Dimers: A Fragmentation−Reconstruction Approach

Ivo Cacelli,[†] Antonella Cimoli,[†] and Giacomo Prampolini*[,†,‡]

Dipartimento di Chimica e Chimica Industriale, Università degli Studi di Pisa, via Risorgimento 35, I-56126 Pisa, Italy, and Scuola Normale Superiore, piazza dei Cavalieri 7, I-56126 Pisa, Italy

Received March 30, 2010

Abstract: A novel approach for exploring the energy minima of the potential energy surface of large and flexible van der Waals dimers is proposed and tested. The total dimer energy is divided into intra- and intermolecular contributions, which can be computed at different levels of theory. The intermolecular energy, which is the time-consuming part of the calculation, is computed by means of the fragmentation reconstruction method (FRM), making possible the calculation of the interaction energy of large molecules. The method is validated by performing geometry optimizations through a quasi-Newton technique on two benchmark medium-sized systems, where the comparison with a direct *ab initio* calculation is still computationally feasible. In both cases, good agreement is achieved between geometries and energies of the resulting energy minima.

1. Introduction

van der Waals (vdW) interactions[1−5] are known to play a relevant role in many different fields of science, ranging from soft matter[6−9] to biochemistry,[10−12] and from molecular recognition[13] to nanotechnologies[14−16] and astrobiology.[17] Nevertheless, for molecular dimers of medium to large dimensions, the accurate calculation of such interactions with standard quantum mechanical (QM) or *ab initio* methods still remains a grand challenge. The main reason for these difficulties arises from the purely quantum mechanical nature of the vdW interactions, which strongly relies on a correct representation of the dynamical electron correlation. For this reason, within the *ab initio* methods, one has to employ post-Hartree−Fock (HF) techniques, whose computational costs dramatically increase along with molecular dimensions. This picture is made even worse when dealing with flexible molecules, whose isolated equilibrium conformation can be altered by the intermolecular interactions. In these cases, dimer energy minimizations should not be performed in a rigid monomer geometry approximation. Moreover, soft matter is characterized[6−8] by molecular and collective conformational changes driven by thermal fluctuations, and an accurate sampling of several local energy minima is therefore required to spot the most probable dimer conformations. A striking example of such features can be found even in a relatively small molecule such as biphenyl, where the torsional angle between the two phenyl rings assumes different values according to the phase (crystal, liquid, or gas) in which it is measured (see ref 18 and references therein). In more complex systems, for instance polymers, liquid crystals, or protein−ligand complexes, the determination of the most stable dimer structures is of fundamental importance in the understanding of the condensed phase properties. A straightforward route to accessing this information could be the use of molecular mechanics (MM), which is often adopted in the case of biomolecular dimers and allows for the computation of very large molecules. Unfortunately, it has recently been shown[19−21] that literature force fields are not able to provide dimer structures in agreement with reference QM data for a large variety of systems.

To overcome the computational problems of QM calculations on large vdW molecules, several fragmentation-based

* To whom correspondence should be addressed. E-mail: giacomo@dcci.unipi.it.

[†] Universita degli Studi di Pisa.

[‡] Scuola Normale Superiore.

10.1021/ct100172w © 2010 American Chemical Society
Published on Web 07/12/2010

strategies have been proposed[22−32] that essentially rely on the possibility of dividing the whole system into small subsystems and performing the calculations for each subsystem. Among these, the fragment molecular orbital (FMO) method[29] and the fragmentation reconstruction method (FRM)[22−24] were devised to account for dispersion energy, whereas other approaches are either coupled with calculations at the HF or DFT level[25,26] or implemented for monomer optimizations.[27,28] To the best of our knowledge, large dimer optimizations were performed only in the FMO approach,[30,33,34] but unfortunately gradients are not yet implemented in FMO coupled with post-HF methods. Furthermore, in all cases, dimer geometry optimizations were performed in a rigid monomer approach.

In this paper, we report a novel approach, based on the FRM[22−24] route to intermolecular energy previously developed in our group, that can be used to study vdW complexes by optimizing the relative position as well as the intramolecular geometry of each monomer, at least for the most flexible internal coordinates. This approach has been implemented in original software code written by us and named POLDO and is able to perform geometry optimizations of large and flexible vdW dimers otherwise impracticable with standard methods. On the other hand, even if FRM reduces the dimensions of the problem (with respect to the whole dimer), a reasonable compromise between accuracy and computational cost is still a major requirement, in view of the large number of calculations possibly involved in a dimer geometry optimization.

In the past decade, along with the impressive development of the computational resources, several groups have reported highly accurate calculations for model $\pi\cdots\pi$ interacting systems. Among others, the groups of Tsuzuki,[35,36] Hobza,[12,20,37,38] and Sherrill[21,39−44] have reported interaction energies at the CCSD(T) level, extrapolated at the complete basis set limit, which is now often referred to as the "gold standard" of quantum chemistry. The major drawback of this approach is the extremely high computational cost of the CCSD(T) method, which scales approximatively as N^7, making calculations rapidly unfeasible with the increase of molecular dimensions. Furthermore, to the best of our knowledge, no geometry optimization at this level of theory has yet been reported in the literature. Computational convenience would rather suggest resorting to a cheaper method, either density- or wavefunction-based.

The methods based on density functional theory (DFT) are generally less expensive. Unfortunately, none of the standard density functionals was shown to be able to reproduce even benzene dimer interaction curves at a qualitative level[45,46] because of an incorrect evaluation of dispersion contribution. Only recently did Truhlar and Zhao[47−49] succeed in reparameterizing the DFT functional (M06-2X) in order to take dispersion into account, achieving a reasonable agreement[49,50] with reference data for benchmark systems. However, very recent results[38] have put into evidence some defects in the overall representation of the computed interaction energy curves. In the same paper,[38] somewhat better performance was reported for the dispersion corrected DFT-D approach, where the standard DFT energy is corrected with an empirical term[43,44,51,52] to reproduce most of the dispersion interaction energy of aromatic dimers.

Finally, among mixed DFT-wavefunction techniques, it is worth mentioning that the SAPT-DFT approach has been shown[38,53,54] to yield results in good agreement with the most accurate *ab initio* values. However, despite its scaling properties with both the molecular dimensions and basis sets being more favorable than CCSD(T) methods,[53] this approach is still computationally too expensive for its straightforward application to the calculation of large vdW dimers.

As far as the wavefunction-based methods are concerned, a computationally convenient post-HF method is the Møller−Plesset second order perturbation (MP2) theory. Besides its affordable costs, another advantage relies in the availability of the energy gradients, which can be straightforwardly used in the POLDO code. On the other hand, a major drawback of the MP2 method is the remarkable overbinding found for aromatic interactions,[35,36,43,55−57] when large basis sets are employed. To overcome this lack, a few MP2-based methods have been recently proposed. Among these, the spin-component-scaled MP2 (SCS-MP2)[58] has been recently compared to CCSD(T) reference values for model systems,[43,57] resulting in a good agreement for $\pi\cdots\pi$ interactions but not for H-bonded systems. The scaled MP3 method (MP2.5)[57] appears to be more accurate, but the computational cost of this method is about 1 order of magnitude higher than standard MP2. A promising method,[59] which combines MP2 and time-dependent TDDFT response theory, was proposed to improve the agreement with the reference data on a set of benchmark aromatic dimers, at a computational cost slightly higher than standard MP2. However, it is worth noticing that the best agreement was obtained making use of rather large basis sets. An alternative choice is the adoption of the standard MP2 method, coupled with a small basis set (6-31G*), where the polarization exponent has been modified to a smaller value (0.25 instead of the standard 0.80) and therefore named 6-31G*(0.25).[60] The comparison with more expensive computational methods, recently reported for molecular complexes with stacking interactions,[19,38,61,62] is positive, since the intermolecular energy overestimation found with larger basis sets is avoided. The MP2/6-31G*(0.25) method was successfully employed by our group in sampling the QM PES of several dimers, among which are benzene[19] and 4-*n*-pentyl,4′cyano-biphenyl (5CB),[22,63] a common mesogenic molecule. In the last case, MP2/6-31G*(0.25) calculations were performed in the FRM scheme.

In this paper, the dimer geometry optimizations are performed with the POLDO code, which uses the FRM approach at the MP2/6-31G*(0.25) level. To test and validate the proposed method, two benchmark medium-sized molecules are chosen, namely, biphenyl and 5CB. The former can be fragmented into benzene moieties for which MP2/6-31G*(0.25) has already been validated. Moreover, its molecular dimensions allow us to perform direct (i.e., without fragmenting) optimizations at the same level of theory that are used to validate the proposed procedure. 5CB is one of the smaller prototypes of vdW dimers containing three

different moieties, namely, aromatic (phenyl), substituted aromatic (cyano-phenyl), and aliphatic (pentyl) bricks. The paper is organized as follows: Section 2 contains the method, theory, and main computational details. The results of POLDO optimizations are discussed in section 3, whereas main conclusions are collected in the last section.

2. Methods and Computational Details

2.1. Dimer Optimizations. The absolute energy E_{tot} of a vdW A···B dimer can be expressed as

$$E_{tot}(AB) = \Delta E(AB) + E(A_0) + E(B_0) \quad (1)$$

where the labels A_0 and B_0 indicate the monomers in their isolated minimum energy conformations, whereas AB stands for the dimer geometry. As the last two terms of eq 1 are constant, the geometry is optimized considering the ΔE(AB) term, which can be seen as the sum of two separate parts, namely an intermolecular (ΔE_{inter}(AB)) and an intramolecular (ΔE_{intra}(AB)) contribution:

$$\Delta E(AB) = \Delta E_{intra}(AB) + \Delta E_{inter}(AB) \quad (2)$$

where

$$\Delta E_{intra}(AB) = [E(A) - E(A_0)] + [E(B) - E(B_0)] \quad (3)$$

and

$$\Delta E_{inter}(AB) = E(AB) - E(A) - E(B) \quad (4)$$

The main reason for considering two distinct contributions in eq 2 is that accurate calculation of ΔE_{intra} and ΔE_{inter} presents a different level of difficulty, and in the proposed approach they are therefore computed in different ways. The former term may be evaluated employing standard QM techniques or by a suitable and accurate MM intramolecular force field. In this last case, only the internal geometrical degrees of freedom to be optimized need to be included in the set of intramolecular coordinates. Conversely, the intermolecular term ΔE_{inter} is computed using the FRM approach, which includes the counter poise (CP) correction[64] to the basis set superposition error (BSSE).

The minimization of E_{tot}(AB) vs the geometrical degrees of freedom has been performed with the POLDO program. POLDO is a FORTRAN code written by the authors and is freely available upon request. The geometrical quantities taken into account are the following:

(1) The translational vector $\vec{R} \equiv (X, Y, Z)$, connecting a defined point of monomer A with a defined point of monomer B. These points may be the monomer barycenter (default choice), a defined atom, or the midpoint of an assigned bond.

(2) Vectors $\vec{\Omega}_i \equiv (\alpha, \beta, \gamma)$ of each monomer i. $\vec{\Omega}_i$ (i = A, B) defines the absolute orientation of one monomer in a fixed reference frame through the three Euler angles α, β, and γ. The rotation center is a point defined within each monomer. As the internal geometry of both monomers can change during the optimization path, the values of the Euler angles are not sufficient to describe the effective rotation of each monomer, and should be merely considered as degrees of freedom. Moreover, since the interaction energy only depends on the reciprocal orientation, six orientational parameters are a redundant set. However, the inclusion in the optimization of Euler angles for both monomers, though not strictly necessary, was found to speed up the convergence toward the absolute minimum.

(3) Vector $\vec{Q}_i$ (i = A, B), containing the internal coordinates of both monomers. Although POLDO can handle in principle any type and number of coordinates, it can sometimes be preferable[65] to optimize only "soft" degrees of freedom, i.e., those internal coordinates which exhibit rather flat energy profiles, for instance, torsional angles along σ bonds. Indeed, considering the low values of the interaction energies as compared with the intramolecular contribution, it is expected that in common vdW complexes only the "soft" degrees of freedom can be significantly affected by the presence of the second molecule.

The optimization is performed using a gradient-based technique in which at each step the new geometry is determined by a quasi Newton method. The QM Cartesian gradients are converted to energy derivatives with respect to the chosen degrees of freedom. The needed transformation matrices are computed by numerical techniques using a five point interpolation formula, which assures a sufficient accuracy and avoids singularities connected with the use of analytical derivatives involving quaternion, in the case of rotational motion. In particular, for the derivative with respect to the translational degrees of freedom, in which the A monomer is fixed in space and B is moved, one has

$$\frac{\partial E_{tot}}{\partial I} = \sum_{i \in B} \left(\frac{\partial(\Delta E_{inter}(AB))}{\partial r_i} \right) \left(\frac{\partial r_i}{\partial I} \right); \quad I = X, Y, Z \quad (5)$$

where r_i ($i = 1, ..., 3N_B$) are the Cartesian coordinates of the atoms belonging to the molecule B formed by N_B atoms. Similarly, for the rotational degrees of freedom

$$\frac{\partial E_{tot}}{\partial \alpha_{B(A)}} = \sum_{i \in B(A)} \left(\frac{\partial(\Delta E_{inter}(AB))}{\partial r_i} \right) \left(\frac{\partial r_i}{\partial \alpha_{B(A)}} \right) \quad (6)$$

and analogous equations hold for β and γ. Finally, the gradients for an internal coordinate $Q_{A(B)}$ of the molecule A(B) is computed by

$$\frac{\partial E_{tot}}{\partial Q_{A(B)}} = \sum_{i \in A(B)} \left(\frac{\partial E(A(B))}{\partial r_i} \right) \left(\frac{\partial r_i}{\partial Q_{A(B)}} \right) + \sum_{i \in A(B)} \left(\frac{\partial(\Delta E_{inter}(AB))}{\partial r_i} \right) \left(\frac{\partial r_i}{\partial Q_{A(B)}} \right) \quad (7)$$

As many of the internal coordinates are kept frozen, the dummy index i in eq 7 runs over all atoms involved in a change of the $Q_{A(B)}$ coordinate and not only over those involved in its definition. For instance, for biphenyl (see next section), the only internal coordinate $Q_{A(B)}$ chosen for optimization is the inter-ring dihedral angle $\phi_{A(B)}$. In this case, the transformation matrix $(\partial r_i/\partial \phi_{A(B)})$ is computed numeri-

cally by small rigid rotation $\delta\phi_{A(B)}$ of all atoms of the rings and detecting the corresponding changes δr_i.

The POLDO code is interfaced with the Gaussian 03[66] software and automatically starts a Gaussian run for each QM calculation. The full minimization proceeds through the following steps:

(1) The energy of each isolated monomer is optimized with respect to all its internal coordinates using the method chosen for the intramolecular contribution and reference energies, $E(A_0)$ and $E(B_0)$, are recovered.
(2) The energy of each monomer at the starting geometry, $E(A)$ and $E(B)$, is computed with the same method chosen for step 1. POLDO recovers energies and relative Cartesian gradients and computes the $\Delta E_{intra}(AB)$ contribution according to eq 3.
(3) POLDO builds all the Gaussian input files needed by the FRM calculation (see the next section for details). Thereafter, all QM runs are automatically performed. Finally, all of the resulting energies and Cartesian gradients are recovered from Gaussian output files and combined in order to reconstruct the FRM interaction energy term $\Delta E_{inter}(AB)$.
(4) The full energy E_{tot} is computed as a sum of internal and intermolecular contributions according to eqs 1 and 2.
(5) All Cartesian gradients are converted into derivatives with respect to the chosen degrees of freedom, and the Hessian matrix is updated for the current geometrical arrangement.
(6) A new set of coordinates is computed according to the Newton−Raphson algorithm. If the total energy gradient and the computed displacements are small enough, the program ends.
(7) Steps 2−4 are repeated with the new geometry. If the total energy decreases, POLDO proceeds through steps 5 and 6; otherwise POLDO performs a line search in the direction of the predicted displacement and goes back to step 2.

2.2. FRM Calculations. The FRM[22−24] was originally developed in our group to calculate the interaction energy of large molecules. It basically relies on the hypothesis that the interaction energy of a vdW dimer can be approximated to a good level of accuracy as a sum of energy contributions between each pair of fragments into which the two monomers can be decomposed. The basic criterion behind this fragmentation scheme is that the ground state electronic density around the atoms of each fragment has to be as close as possible to that around the same atoms in the whole molecule. The main advantage of this approach lies in the possibility of performing calculations between moieties much smaller than the whole molecules under study. In previous applications,[23,24,63,67] this has allowed us to include electronic correlation effects and to obtain a good estimate of the dispersion energy which accounted for a large fraction of the attractive intermolecular energy of the considered dimers. The information gained about the interaction energy between the fragments pairs is then used to set up the full intermolecular energy.

The first step of the FRM is a decomposition of the whole molecule into moieties by fragmenting it along properly chosen bonds. The valence of the resulting fragments is then saturated by suitable atoms or small groups named "intruders." The intermolecular energy is thereafter expressed as a sum of the energy contributions arising from all of the fragment pairs. It is worth mentioning that, in order to recover the total dimer interaction energy, the intruder groups have to be subsequently canceled from the whole dimer and their energy contributions properly subtracted. More details about FRM can be found in the original papers.[22,24]

2.3. Computational Details. All isolated monomer calculations (eq 3) were performed at the DFT level of theory, using the B3LYP functional with a correlation consistent cc-pVDZ basis set. In the case of biphenyl, the intramolecular contribution $E(k)$ (k = A, B) was computed at the MM level, using the following expression for the inter-ring dihedral:

$$E(k) = \sum_n C_n(1 + \cos(n\phi_k)); \quad k = A, B \tag{8}$$

where all the remaining internal coordinates are fixed at their equilibrium values. The set of force-field parameters C_n was taken from ref 18, where they were derived from accurate QM calculations.

All FRM fragment−fragment calculations were performed at the MP2/6-31G*(0.25) level, in the supermolecule approach and corrected for the BSSE with the CP correction. Consequently, all MP2 direct optimizations and single point calculations, performed on the whole dimers, were correspondingly computed with the same basis set and CP corrected.

3. Results and Discussion

3.1. MP2/6-31G*(0.25) Validation. A mandatory test for vdW dimer optimizations is the validation of the level of theory to be used for the intermolecular energy calculations. It is worth pointing out that large and flexible vdW dimers may exhibit several energy minima, in which their reciprocal arrangements can be very different from simple stacked geometries. For this reason, all methods should be evaluated in several geometries, where, for instance, both $\pi\cdots\pi$ and $H\cdots\pi$ interaction types play different roles. The benzene dimer is a good candidate for this validation, as it can be considered as a prototype of vdW interactions, and at the same time, its dimensions allow high-level reference calculations.

To this aim, MP2/6-31G*(0.25) data are computed and results validated vs those of refs 43 and 44, where a detailed comparison among several methods has been reported for different geometries of the benzene dimer. Indeed, in these papers, Sherrill and co-workers report the interaction energy curves for sandwich (SW), T-shaped (TS), and parallel displaced (PD) benzene dimers at the CCSD(T) level, extrapolated at the complete basis set limit (CCSD(T)/CBS), which can be considered the reference values. In Figure 1, some of those curves are shown and compared with those obtained in this work using the MP2 method with the modified 6-31G*(0.25) basis set.

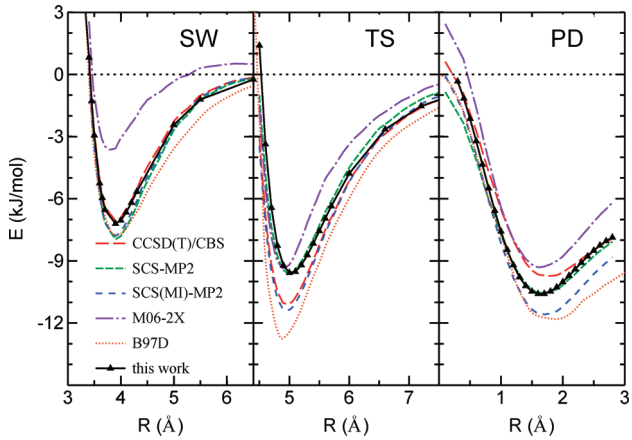

Figure 1. Interaction energies for sandwich (SW), T-shaped (TS), and parallel displaced (PD) arrangements of the benzene dimer at different levels of theory. All energies were taken from refs 43 and 44 where dimer geometries are described in detail (PD displacement is 3.4 Å). In this work, the same curves have been calculated at the MP2/6-31G*(0.25) level and reported with triangles in the above figure.

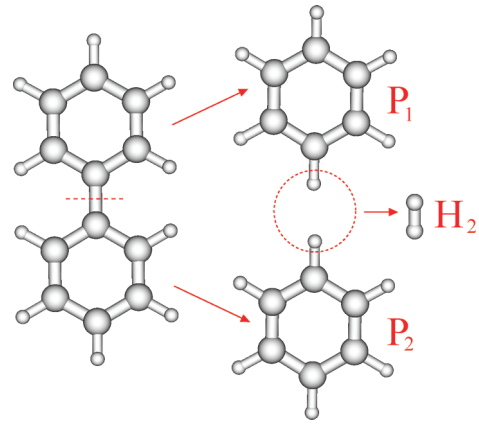

Figure 2. Fragmentation scheme for biphenyl. P_1 and P_2 are two benzenes, and H_2 is the intruder molecule. In the above picture, both moieties and intruder molecule have been shifted (red arrows) only for the sake of clarity (see text). For instance, both H atoms of the intruder molecole H_2 lie on the C−C bond connecting the two aromatic moieties. These moieties will be labeled with a further subscript A or B (that is $P_{1A(B)}$, $P_{2A(B)}$, $H_{2A(B)}$) depending on which of the two biphenyl monomers they belong.

Besides maintaining the correct relative order (i.e., $E_{TS} \simeq E_{PD} < E_{SW}$), MP2/6-31G*(0.25) shows an overall good agreement with the reference data: the accord is quantitative for the SW arrangement, whereas it slightly overestimates and underestimates CCSD(T)/CBS binding energies for PD and TS geometries by ∼0.9 and ∼1.5 kJ/mol, respectively. As far as the intermolecular separation at the minimum is concerned, a good agreement results for all geometries. Most important, the comparisons reported in refs 43 and 44 show that all other methods taken into account perform either worse or comparably. Therefore, at least for the benzene dimer, the MP2/6-31G*(0.25) method seems a good compromise between accuracy and computational cost (also considering the large number of calculations requested in an optimization procedure).

3.2. Biphenyl. After some preliminary tests (whose results are reported as Supporting Information), the first validation of the proposed procedure was attemped on the biphenyl molecule, one of the smaller prototypes of a fragmentable vdW dimer. Biphenyl is composed of two phenyl moieties (P_1 and P_2, see Figure 2) connected by a quasi-σ bond, seeing that the dihedral angle ϕ between the two rings is ∼42° in the gas phase.[18]

The intramolecular contribution, ΔE_{intra}, was computed at the MM level according to eq 8. As far as the intermolecular energy is concerned, the FRM scheme was applied to each biphenyl monomer by a cut along the inter-ring bond (see Figure 2). Indeed, this is the only possible fragmentation choice that respects the electronic density criteria exposed in the previous section. H atoms were then added to saturate the valence of the resulting C_6H_5 moieties, as shown in Figure 2. It is worth noticing that the spatial positions of the fragments are unchanged with respect to the whole molecule, and the location of the intruders H_{2A} and H_{2B} is unambiguously determined by the internal geometry of the saturated fragments. In other words, the Cartesian coordinates of all atoms in the fragments are unchanged with respect to the ones in the whole molecule, resulting in a slightly altered H_2 bond distance (0.68 Å, instead of the equilibrium value of 0.74 Å). The intermolecular energy of the whole biphenyl dimer is thus made up of the following contributions (see Figure 2):

$$\Delta E_{inter}(AB) = \underbrace{\Delta E(P_{1A}\cdots P_{1B}) + \Delta E(P_{1A}\cdots P_{2B}) + \Delta E(P_{2A}\cdots P_{1B}) + \Delta E(P_{2A}\cdots P_{2B})}_{PhH\cdots PhH} - \underbrace{(\Delta E(H_{2A}\cdots P_{1B}) + \Delta E(H_{2A}\cdots P_{2B}) + \Delta E(P_{1A}\cdots H_{2B}) + \Delta E(P_{2A}\cdots H_{2B}))}_{H_2\cdots PhH} + \Delta E(H_{2A}\cdots H_{2B}) \quad (9)$$

where $\Delta E(i_A\cdots j_B)$ is the interaction energy between fragment i, belonging to A, and fragment j, belonging to B.

The starting geometry was created by randomly displacing the B monomer and setting both ϕ's at 28°, as shown in Figure 3; the energy of the obtained arrangement is −10.8 kJ/mol, resulting from a sum of $\Delta E_{inter} = -15.4$ kJ/mol and $\Delta E_{intra} = 4.0$ kJ/mol. Given the reduced flexibility of the ring internal coordinates, this dimer conformation was optimized with the POLDO software by varying the translational ($\vec{R}$) and rotational ($\vec{\Omega}_B$) sets of coordinates together with both internal dihedrals ϕ_A and ϕ_B. The most striking feature during optimization is the rapid decrease to 0° of the β_B angle, which indicates a tendency of the two biphenyl monomers to realign their *para* axes, thus maximizing the $\pi\cdots\pi$ interactions. The inclusion of translational degrees of freedom allows the molecules to move along Y, reducing their distance to 3.6 Å, with a small displacement (−1.7 Å) along the X direction. Finally, the torsional dihedrals both reach the equilibrium value, found for the isolated monomer. The result is a local dimer minimum, almost isoenergetic (−31.5 kJ/mol vs −32.9 kJ/mol) with that found in preliminary optimizations (see test 2 in the Supporting Information), where the biphenyl long axes were imposed to be parallel. Some relevant geometrical data of the final optimized dimer are reported in Table 1.

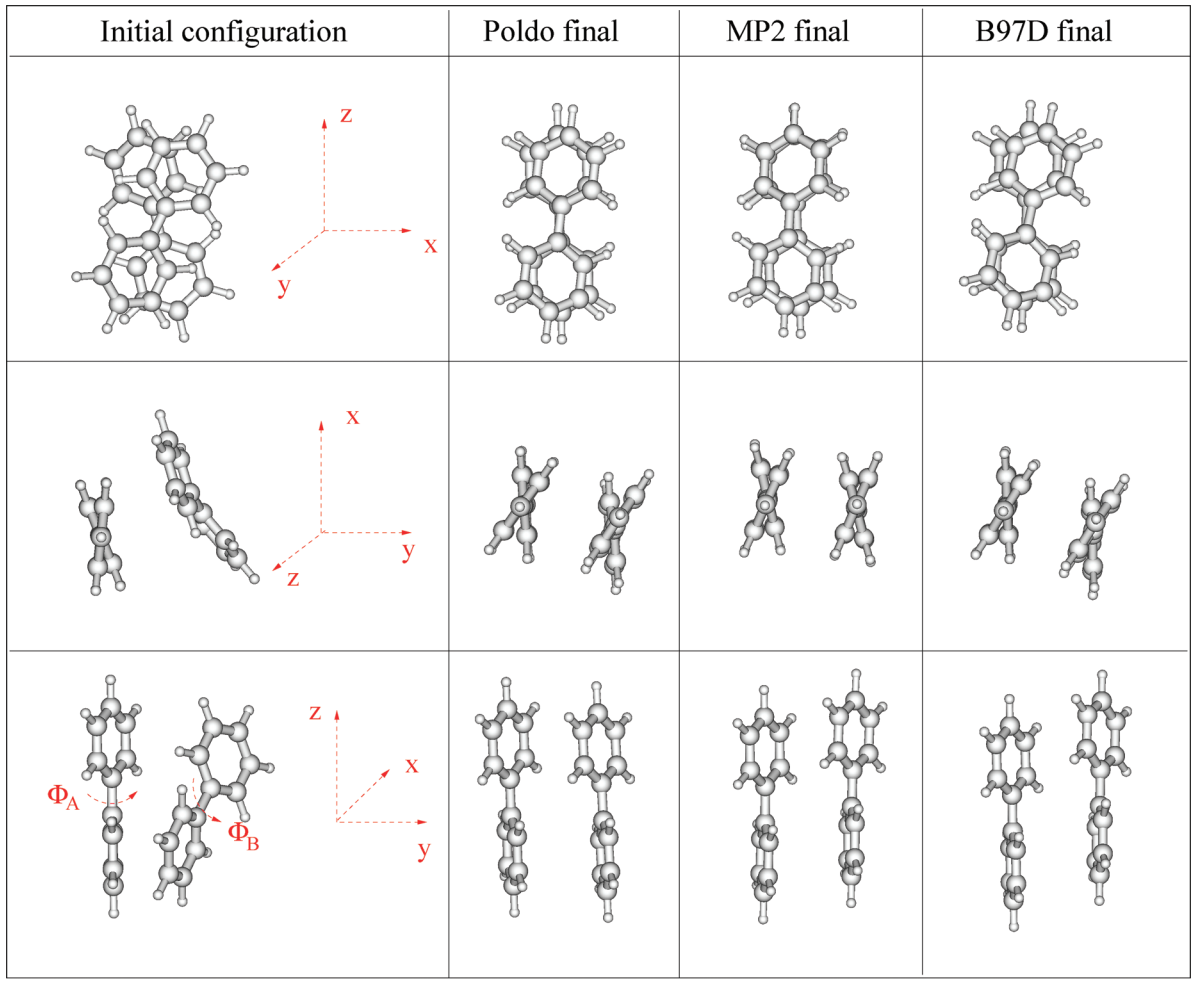

Figure 3. Complete optimization of a randomly placed biphenyl dimer. Starting (left column) and POLDO optimized (second column) geometries are shown from different points of view. The third and fourth columns refer to MP2 and B97D direct optimizations of the whole dimer, respectively.

Table 1. Optimized Biphenyl Dimer: Total Energy and Geometrical Values Obtained with Direct MP2 (second column), POLDO (third column), and B97D Optimizations

	Direct MP2	POLDO	B97D
ϕ_A	37.0°	40.0°	34.4°
ϕ_B	37.0°	40.0°	34.6°
$H_4^A\widehat{C_1^AC_1^B}H_4^B$	4.6°	8.0°	9.6°
$H_4^AH_4^B$	3.85 Å	4.04 Å	3.91 Å
$H_{4'}^AH_{4'}^B$	3.84 Å	3.62 Å	3.92 Å
$C_4^AC_4^B$	3.81 Å	3.97 Å	3.87 Å
$C_{4'}^AC_{4'}^B$	3.80 Å	3.64 Å	3.88 Å
$C_1^AC_1^B$	3.70 Å	3.81 Å	3.79 Å
$C_{1'}^AC_{1'}^B$	3.70 Å	3.74 Å	3.79 Å
$E(AB)$	-34.2 kJ/mol	-31.5 kJ/mol	-31.2 kJ/mol

As biphenyl molecular dimensions still allow for an MP2 direct optimization on the whole dimer, this was performed for comparison purposes and for the validation of our method. The direct MP2 optimization was performed starting from the final POLDO geometry, and each optimization step was CP corrected for BSSE. The final energy found with the direct MP2 route is −34.2 kJ/mol: 2.7 kJ/mol more attractive with respect to the minimum computed by our algorithm. This small difference can be ascribed to the different level of theory used for ΔE_{intra} and to small rearrangements of the internal geometry which are allowed in direct MP2 but not in POLDO. It is worth stressing that this energy difference cannot be attributed to FRM inaccuracies, as the direct MP2 energy of the final geometry obtained by POLDO is −31.9 vs −31.5 kJ/mol. A further test was performed by optimizing the whole biphenyl dimer using a DFT-D technique, namely, the B97D functional with the TZV2P basis set as first proposed by Grimme.[52] Although, up to our knowledge, the B97D functional was never employed for the biphenyl dimer, the performances of this dispersion corrected approach were recently tested[44] on the benzene dimer, giving results comparable with the MP2/6-31G*(0.25) method, as reported in Figure 1. In fact, if a B97D calculation is performed on the final geometry optimized by POLDO, an intermolecular energy of −29.7 kJ/mol is found. Conversely, the final optimized energy found with this method is −31.2 kJ/mol, not far from the direct MP2 value, and very close to the one obtained with the POLDO procedure.

In Table 1, geometrical values obtained with the direct MP2 and B97D optimizations are reported for comparison, while in Figure 3, POLDO, direct MP2, and B97D final geometries are sketched in the second, third, and fourth columns, respectively. Notwithstanding the good agreement

Table 2. Fragment−Fragment Energy Contributions (kJ/mol) in the POLDO Optimization of the Biphenyl Dimer[a]

Fragments $i_A \cdots j_B$		ΔE_{inter}	ΔE^{HF}_{inter}
$P_{1A} \cdots P_{1B}$	(PD)	−9.70	26.72
$P_{2A} \cdots P_{2B}$		−10.67	18.06
$P_{1A} \cdots P_{2B}$	(CD)	−4.59	−0.07
$P_{2A} \cdots P_{1B}$		−5.71	2.02
$H_{2A} \cdots H_{2B}$		0.05	0.09
$P_{1A} \cdots H_{2B}$		0.01	0.36
$P_{2A} \cdots H_{2B}$		0.41	0.88
$H_{2A} \cdots P_{1B}$		0.42	0.94
$H_{2A} \cdots P_{2B}$		0.03	0.35
Biphenyl - Biphenyl		-31.51	49.35

[a] The second and third column report intermolecular MP2 and HF energies, respectively.

among the three energy values, the final optimized geometries show some minor differences, suggesting that the PES around the minimum is rather flat. All algorithms predict a nonplanar value for ϕ_A and ϕ_B and an intermolecular distance between 3.7 and 3.9 Å, seeing that the biphenyl *para* axes are slightly more aligned in the dimer optimized with the direct MP2 algorithm. Indeed, an estimate of how much the A and B long axes are collinear can be gained by measuring the dihedral angle defined by the quadruplet of atoms $H_4^A-C_1^A-C_1^B-H_4^B$. The latter goes from an initial value of 38° to a final one of 5°, 8°, and 10° in the direct MP2, POLDO, and B97D optimized geometries, respectively.

Within the FRM, the intermolecular energies of all fragment pairs are directly available and can be used to get a deeper insight into the forces driving the optimization. Referring to the fragment labels defined in Figure 2, it can be seen that in the final geometry the benzenes of A and B are in parallel (PD) and cross-displaced (CD) arrangements. In Table 2, energy contributions for all fragment pairs are reported.

From these values it results that, notwithstanding that the major contribution comes from the PD arrangements, the moieties placed in CD geometries do not give a negligible contribution to the intermolecular energy.

4. 5CB

As a second benchmark calculation, the 5CB dimer was chosen. In this case, both intra- and intermolecular energies were computed with QM methods. The intramolecular energy was evaluated at the DFT level (B3LYP/cc-pVDZ). The intermolecular calculations were performed according to the fragmentation pattern described in the following and reported in Figure 4, and using the MP2/6-31G*(0.25) level of theory for the fragment−fragment interaction energies. Each 5CB monomer is fragmented by a cut along the inter-ring bond and the aromatic−aliphatic linkage. The valence of all fragments is saturated with H atoms, obtaining for each monomer three moieties (cyano-benzene, benzene, and *n*-pentane) and two H_2 intruder molecules.[63]

Energy minima were searched starting from different configurations. According to the mutual orientation of the two molecular long axes (which can be considered approximatively as lying along the cyano−biphenyl *para* axis), the

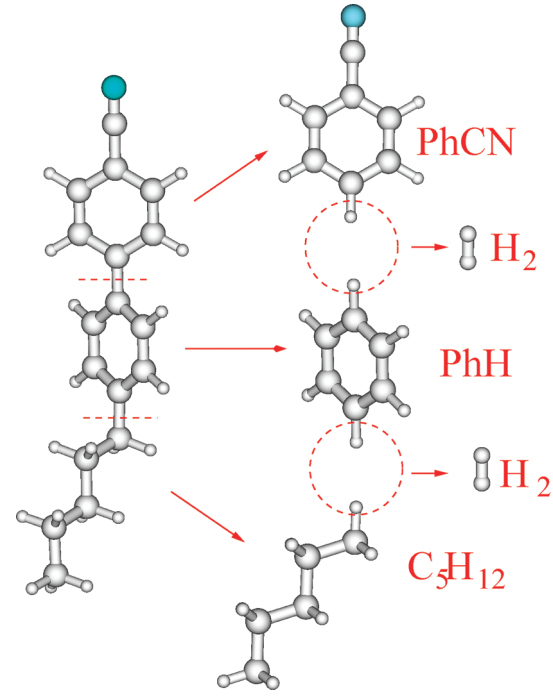

Figure 4. 5CB fragmentation scheme. All moieties will be labeled with a subscript A or B (i.e., $PhH_{A(B)}$) depending on which of the two 5CB monomers they belong to.

Table 3. 5CB, Summary of Optimized Energies for the Considered Arrangements[a]

geometry	ΔE(AB)	ΔE_{intra}(A)	ΔE_{intra}(B)	ΔE_{inter}(AB)
PFF1	−44.40	0.77	1.30	−46.47
PFF2	−47.23	0.79	2.85	−50.87
PSF	−31.05	0.37	0.04	−31.46
PD	−39.86	0.00	0.00	−39.86
An	−51.16	0.33	0.02	−51.51

[a] All energies are in kJ/mol.

investigated geometries can be referred to as parallel (P: long axes pointing in the same direction) or antiparallel (An: they point in opposite directions) arrangements. Among all possible P dimers, face-to-face (PFF) and side-to-face (PSF) and displaced (PD) geometries were investigated. In the PFF case, the aromatic rings of the two monomers are in a sandwich spatial disposition, whereas in the PSF they are found in a T-shaped geometry. Parallel displaced geometries were instead obtained from PFF by displacing one monomer along its long axis. Final energy contributions and selected geometrical quantities for all investigated arrangements are summarized in Tables 3 and 4, respectively.

PFF1 and PFF2 arrangements were obtained as shown in Figure 5 and are described in the following. Two 5CB monomers, in their isolated optimized conformation, were superimposed, and monomer B was then shifted by 5.5 Å along the vector normal to the central ring plane. Thereafter an, $\alpha_B = 180°$ rotation was performed and the obtained dimer geometry labeled PFF1 (geometry a in Figure 5). During optimization, PFF1 turns into a sort of PD arrangement: the aromatic rings come nearer, but a displacement takes place along the long molecular axis and the *X* direction (see Figure 5). In the final (geometry b in Figure 5) configuration, 5CB long molecular axes are not parallel anymore, and the

Table 4. Characterization of the Resulting 5CB Dimer Minima by Selected Geometrical Quantities[a]

	PFF1	PFF2	PSF	PD	An
$\phi_A - \phi_B$	29.0 - 30.0	30.0 - 27.0	31.8 - 37.5	34.0 - 33.0	32.0 - 34.0
$C_1^A\widehat{C_{1'}^A C_{1'}^B} C_1^B$	-20.7	-31.4	-24.0	13.7	-14.7
N-N	4.2	4.8	6.4	5.95	13.6
C_4-C_4	3.8	4.1	5.7	5.7	3.7 (C_4-$C_{4'}$)
C_1-C_1	3.7	3.7	5.1	5.4	3.7 (C_1-$C_{1'}$)
$C_{1'}$-$C_{1'}$	3.7	3.8	4.9	5.2	3.7 ($C_{1'}$-C_1)
$C_{4'}$-$C_{4'}$	3.9	4.3	4.7	5.0	3.9 ($C_{4'}$-C_4)

[a] Angle are reported in degrees and distances in Å.

dihedral angle defined by the quadruplet $C_1^A-C_{1'}^A-C_{1'}^B-C_1^B$ changes from 0° to 20°. A possible cause of this rotation may be the CN dipole−dipole repulsion. As far as dihedral angles are concerned, it is interesting to note that inter-ring (ϕ) values are different from the ones computed in the gas phase (∼42°) but similar to those expected in the condensed phase[68] (∼30°). Conversely, no conformational changes are induced in side chains by dimer interactions. The total energy of the dimer, $E_{tot}(AB)$, decreases from −17.5 to −44.4 kJ/mol, seeing that A's and B's intramolecular energies are 0.8 and 1.3 kJ/mol, respectively, with $\Delta E_{inter}(AB) = -46.5$ kJ/mol. As reported in Table 5, FRM again correctly reconstructs the interaction energy since an MP2 direct calculation, performed on the final POLDO optimized whole dimer geometry, gives $\Delta E_{inter}(AB) = -47.5$ kJ/mol.

The most relevant fragment−fragment contributions to ΔE_{inter} are reported in Table 5. As expected, the main contributions to the total intermolecular energy come from the $\pi\cdots\pi$ pair interactions. The cyano−benzene pair is found in a PD-like configuration whose large stability is little affected by the repulsive dipole−dipole interaction, due to the aforementioned rotation of the CN groups. The second contribution comes from the benzene pair, which takes advantage of the SW to PD displacement.

In the PFF1 optimized geometry, chain−chain interactions do not contribute significantly, as they point in opposite directions. If one of them is rotated by 180° around the 5CB's *para* axis, PFF2 geometry is generated as displayed in Figure 5. After optimization, the chain−chain energy amounts to −5.35 kJ/mol (see Table 5), and since all other fragment pair interactions are little affected by this chain rotation, PFF2 total interaction energy decreases from −46.47 kJ/mol (PFF1-opt) to −50.87 (PFF2-opt).

The next optimization was performed selecting as the starting geometry a PSF arrangement (see Figure 6, left panel) which is characterized by a T-shaped initial disposition of the aromatic rings. Owing to the stability of the T-shaped benzene dimer, an interaction energy comparable with the previous ones might be expected. However, as reported in Table 5, this is not the case. The main reason resides in a reduced stability of the PhCN dimer in the T-shaped configuration with respect to a PD one. On the contrary, the T-shaped benzene pair accounts for the maximum contribution (−8.6 kJ/mol) to the total intermolecular energy. This global lower interaction is consistent with the ϕ_A and ϕ_B values being more close to those of the isolated molecule.

Table 5. 5CB, More Relevant Optimized Fragment−Fragment Contributions to the Dimer $\Delta E_{inter}(AB)$ in Different Geometries[a]

fragment $i_A\cdots j_B$	PFF1	PFF2	PSF	PD	An
PhCN···PhCN	−14.50	−12.97	−7.37	−9.86	−3.54
PhCN···PhH	−7.77	−8.62	−5.95	−0.53	−14.09
PhCN···C_5H_{12}	−0.58	−0.61	−0.44	−0.05	−5.25
PhH···PhCN	−4.86	−5.23	−1.75	−13.75	−14.81
PhH···PhH	−10.36	−9.74	−8.65	−6.56	−6.09
PhH···C_5H_{12}	−2.62	−2.44	−3.39	−0.38	−0.45
C_5H_{12}···PhCN	−0.20	−0.18	−0.13	−2.34	−4.72
C_5H_{12}···PhH	−1.63	−3.27	−1.27	−4.58	−0.42
C_5H_{12}···C_5H_{12}	−1.34	−5.35	−2.62	−1.15	−0.02
$\Delta E_{inter}(AB)$ total	−46.47	−50.87	−31.46	−39.86	−51.51
direct MP2	−47.50	−51.09	−31.63	−40.17	−52.57

[a] In the last row, the MP2 energy computed on the whole POLDO optimized geometry is reported. All energies are in kJ/mol.

A last test on another parallel geometry was devised by displacing the monomer B of PFF1 dimer by ∼4 Å along *Z*, obtaining a PD arrangement. During optimization, a β rotation of B takes place, together with minor translational shifts that bring the C_4 atom of B in front of the $C_{1'}$ of the A monomer. A better comprehension of spatial displacement of A and B can be gained looking at the intermolecular energies of fragment−fragment pairs, as reported in Table 5. Benzene−cyanobenzene pairs contribute −13.75 and −0.53 kJ/mol, since the displacement along *Z* has led the former pair in a stacked conformation and the latter to large distance. The optimized PD dimer is also stabilized by $\pi\cdots\pi$ homodimer interactions (−9.86 and −6.56 kJ/mol) as well as one pentane−cyanobenzene pair (−4.58 kJ/mol). The final interaction energy, $\Delta E_{inter}(AB)$, sums up to −39.86 kJ/mol, showing that the PD optimized geometry is a local minimum more stable than the PSF dimer, but less favorable than the PFF ones.

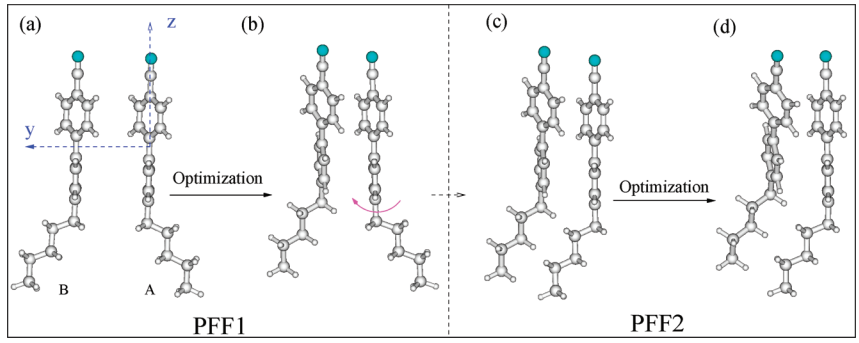

Figure 5. 5CB PFF1 (starting a and final b) and PFF2 (starting c and final d) geometries. Part c was obtained from part b through rotation of the first dihedral of the side chain.

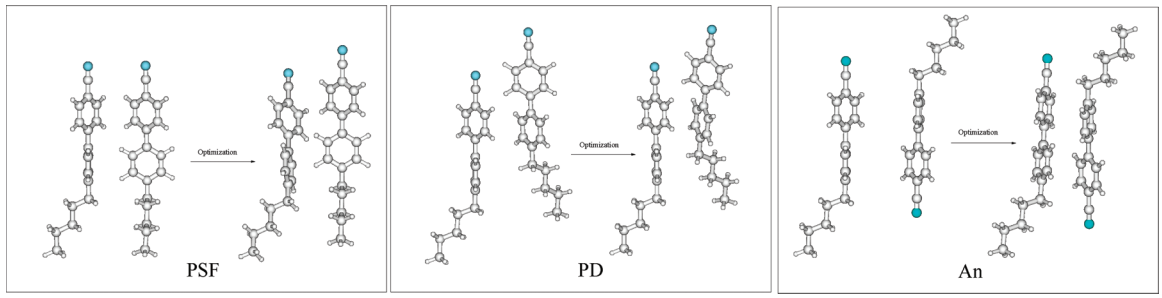

Figure 6. Parallel side-face (PSF, left panel), parallel displaced (PD, central panel), and antiparallel (An, right panel) starting and final geometries.

Finally, an antiparallel (An) 5CB dimer geometry was generated. This configuration is reported in Figure 6, and it was obtained rotating the B monomer of 180° around β and displacing it at 6 Å farther from A, along Y. In this way, the C_4 atom of one molecule faces the $C_{4'}$ of the other, and the C_1 atom of A(B) overlooks the $C_{1'}$ atom of B(A). During the optimization, the Y distance decreases to 3.7 Å, and B is subjected to a small β rotation, causing an imperfect stacking of the aromatic rings in the final configuration. From Table 5, it appears that, due to the antiparallel arrangement and difference from previous cases, the most important contributions are the cyanobenzene−benzene interactions, which each account for ∼−14 kJ/mol. The cyanobenzene and benzene homodimer contributions are much less, whereas the aliphatic−aromatic interactions now play an important role. Once again, side chain dihedrals are not affected by the presence of the second molecule, whereas the inter-ring dihedral is found around 33°. The final interaction energy ΔE_{inter}(AB) is −50.1 kJ/mol, suggesting that, at least for the phase space explored here, dimers of the An type are the most stable conformations. This conclusion seems to be consistent with the experimental observation of 5CB's nematic phases with zero permanent dipole (see ref 69 and references therein). This is an example of how information on dimers can help in a deeper understanding of condensed phase properties: in this case, the origin of the lack of permanent dipole in 5CB condensed ordered phases can, in fact, be tracked down to the greater stability of the antiparallel configuration.

5. Conclusions

In this paper, a new method for accurate geometry optimizations has been presented. The approach is explicitely devised for van der Waals complexes, even of large dimensions, which can be studied at affordable computational costs. This method, implemented in an original code named POLDO, can be used either to search for the most stable configuration or to investigate the relative stability of different local minima, in case one wants to explore some relevant portions of the dimer phase space. The optimization algorithm is guided by the energy gradients and an approximate Hessian, in the framework of the so-called quasi-Newton methods. The pivot of the whole procedure is the fragmentation reconstruction method (FRM), which involves a decomposition of the two molecules of the dimer into smaller fragments, the calculation of the interaction energies of all resulting fragment pairs and the final reconstruction of the whole intermolecular energy, thus avoiding the energy calculation on the entire system. This shortcut heavily cuts down computational costs, allowing calculations on molecules made up of a large number of atoms, that would be otherwise unaffordable.

The method was first tested on the biphenyl dimer, whose dimensions allowed us a comparison with the energy and geometries obtained by an optimization performed directly on the whole dimer. The intermolecular energies computed via FRM and on the whole dimer agree quantitatively (∼0.4 kJ/mol), and at the same time, the computational cost is lowered by almost 4 times. A good accord is also found between POLDO and direct MP2 optimization results, where the difference of 2.7 kJ/mol was ascribed to the different dimensionality of the optimized PES. As a second benchmark, a common nematogenic molecule, whose dimer is formed by 268 electrons, was chosen. The optimization was performed both on intermolecular coordinates and on a reduced set of internal degrees of freedom. As in the previous case, the comparison between FRM and direct (single point) calculations is favorable, seeing that the average error is ∼0.5 kJ/mol. Most important, the ratio of the CPU costs is 5; that is, it becomes more favorable with the increase of the molecular dimensions. It should also be stressed that 5CB dimensions make an MP2 direct optimization almost unfeasible on standard workstations.

In conclusion, the proposed optimization procedure, implemented in the POLDO code, grants some new advantages with respect to full and/or other fragmentation based minimization methods that can be summarized as follows:

(i) Inter- and intramolecular interactions can be treated at different levels of theory. Since the latter type is often less sensitive to the method/basis set employed, this may allow us to save computer time with a negligible loss of accuracy. Moreover, a FF description can also be employed, if accurate potentials are available.

(ii) The intermolecular energy is computed by means of the FRM approach, which does not rely on any specific method/basis set. Although in this and previous papers the FRM approach has been coupled with the MP2/6-31G*(0.25) level of theory, there are no obstacles to joining FRM with other promising methods, accurate while computationally affordable, such as those recently proposed in the literature and detailed in previous sections.

(iii) The fragmentation strategy on which the whole procedure is based allows for a deeper insight into experimental nonaccessible data, as it readily yields detailed information on local fragment−fragment interactions which concur with the formation of the whole vdW dimer.

In the near future, we plan to employ this method in two different contexts. The first one involves the parametrization of intermolecular force fields, suitable for classical computer simulations, from a database built using quantum mechanical calculations. In this context, the fragment−fragment interaction energies and their gradients, provided by FRM calculations, can be added to the database, yielding further information that can be exploited to reduce the redundancy of the FF parameters in the fitting procedure, therefore increasing the robustness of the set of parameters. The second project concerns the geometry optimization of large systems with particular attention to molecules of biological interest. Indeed, this approach allows for taking into account, during the optimization process, selected internal degrees of freedom while retaining a fixed geometry for more rigid parts of the monomer under study. This possibility seems, for instance, to fit the case of nucleobase quadruplets, where the flexibility around H bonds of two base pairs can be taken into account together with the intermolecular separation of the stacked pairs, whereas the planarity of the aromatic rings may be kept frozen during optimization.

Supporting Information Available: Additional text regarding preliminary tests. This material is available free of charge via the Internet at http://pubs.acs.org.

References

(1) Margenau, H.; Kestner, N. R. *Theory of Intermolecular Forces*; Pergamon Press: Braunschweig, Germany, 1969.

(2) Stone, A. J. *The Theory of Intermolecular Forces*; Oxford University Press: Oxford, U. K., 1996.

(3) Kaplan, I. G. The Interatomic Potential Concept and Classification of Interactions. In *Handbook of Molecular Physics and Quantum Chemistry*; Wilson, S., Bernath, P. F., McWeeny, R., Eds.; Wiley: Chichester, West Sussex, England, 2003.

(4) Israelachvili, J. *Intermolecular and Surface Forces*, 3rd ed.; Academic Press: London, 2010.

(5) Parsegian, V. A. *Van der Waals Forces: A Handbook for Biologists, Chemists, Engineers, and Physicists*; Cambridge University Press: Cambridge, U. K., 2005.

(6) Kleman, M.; Laverntovich, O. *Soft Matter Physics An Introduction*; Springer: Berlin, 2003.

(7) Hamley, I. *Introduction to Soft Matter: Synthetic and Biological Self-Assembling Materials*, Revised ed.; Wiley: Chichester, West Sussex, England, 2007.

(8) Collings, P. J.; Hird, M. *Introduction to Liquid Crystals*; Adam Hilger: Bristol, U. K., 1997.

(9) Demus, D.; Goodby, J.; Gray, G. W.; Spiess, H. W.; Vill, V. *Handbook of Liquid Crystals*; Wiley-VCH: Weinheim, Germany, 1998; Vol. 1: Fundamentals.

(10) McGaughey, G. B.; Gagné, M.; Rappé, A. *J. Biol. Chem.* **1998**, *273*, 15458.

(11) Hobza, P.; Sponer, J. *J. Am. Chem. Soc.* **2002**, *124*, 11802.

(12) Sponer, J.; Riley, K.; Hobza, P. *Phys. Chem. Chem. Phys.* **2008**, *10*, 2595.

(13) Meyer, E. A.; Castellano, R. K.; Diederich, F. *Angew. Chem., Int. Ed.* **2003**, *42*, 1210.

(14) Bushby, R.; Lozman, O. *Curr. Opin. Colloid Interface Sci.* **2002**, *7*, 343.

(15) Laschat., S.; Baro, A.; Steinke, N.; Giesselmann, F.; Hagele, C.; Scalia, G.; Judele, R.; Kapatsina, E.; Sauer, S.; Schreivogel, A.; Tosoni, M. *Angew. Chem., Int. Ed.* **2007**, *46*, 4832.

(16) van de Craats, A. M.; Warman, J. M.; Müllen, K.; Geerts, Y.; Brand, J. D. *Adv. Mater.* **1998**, *10*, 36.

(17) Ehrenfreund, P.; Rasmussen, S.; Cleavesand, J.; Chen, L. *Astrobiology* **2006**, *6*, 490.

(18) Cacelli, I.; Prampolini, G. *J. Phys. Chem. A* **2003**, *107*, 8665.

(19) Cacelli, I.; Cinacchi, G.; Prampolini, G.; Tani, A. *J. Am. Chem. Soc.* **2004**, *126*, 14278.

(20) Valdes, H.; Pluháčková, K.; Pitoňák, M.; Řezáč, J.; Hobza, P. *Phys. Chem. Chem. Phys.* **2008**, *10*, 2747.

(21) Sherrill, C. D.; Sumpter, B.; Sinnokrot, M. O.; Marshall, M.; Hohenstein, E.; Walker, R.; Gould, I. *J. Comput. Chem.* **2009**, *30*, 2187.

(22) Amovilli, C.; Cacelli, I.; Campanile, S.; Prampolini, G. *J. Chem. Phys.* **2002**, *117*, 3003.

(23) Amovilli, A.; Cacelli, I.; Cinacchi, G.; De Gaetani, L.; Prampolini, G.; Tani, A. *Theor. Chim. Acc.* **2007**, *117*, 885.

(24) Cacelli, I.; Cimoli, A.; DeGaetani, L.; Prampolini, G.; Tani, A. *J. Chem. Theory Comput.* **2009**, *5*, 1865.

(25) Zhang, D. W.; Zhang, J. Z. H. *J. Chem. Phys.* **2003**, *119*, 3599.

(26) Xiang, Y.; Zhang, D. W.; Zhang, J. Z. H. *J. Comput. Chem.* **2004**, *25*, 1431.

(27) Li, S.; Fang, T. *J. Am. Chem. Soc.* **2005**, *127*, 7215.

(28) Ganesh, V.; Dongare, R.; Balarayan, P.; Gadre, S. *J. Chem. Phys.* **2006**, *125*, 104109.

(29) Fedorov, D.; Kitaura, K. *The Fragment Molecular Orbital Method: Pratical Applications to Large Molecular Systems*; CRC press: Boca Raton, FL, 2009.

(30) Fedorov, D.; Ishida, T.; Kitaura, K. *J. Phys. Chem. A* **2007**, *111*, 2722.

(31) Dahlke, E.; Truhlar, D. *J. Chem. Theory Comput.* **2007**, *3*, 46.

(32) Řezáč, J.; Salahub, D. R. *J. Chem. Theory Comput.* **2010**, *6*, 91.

(33) Chiba, M.; Fedorov, D.; Nagata, T.; Kitaura, K. *Chem. Phys. Lett.* **2009**, *474*, 227.

(34) Li, H.; Fedorov, D.; Nagata, T.; Kitaura, K.; Jensen, J.; Gordon, M. *J. Comput. Chem.* **2010**, *31*, 778.

(35) Tsuzuki, S.; Uchimaru, T.; Matsamura, K.; Mikami, M.; Tanabe, K. *Chem. Phys. Lett.* **2000**, *319*, 547.

(36) Tsuzuki, S.; Honda, K.; Uchimaru, T.; Mikami, M.; Tanabe, K. *J. Am. Chem. Soc.* **2002**, *124*, 104.

(37) Hobza, P.; Zahradník, R.; Müller-Dethlefs, K. *Collect. Czech. Chem. Commun.* **2006**, *71*, 443.

(38) Riley, K.; Pitoňák, M.; Černý, J.; Hobza, P. *J. Chem. Theory Comput.* **2010**, *6*, 66.

(39) Sinnokrot, M. O.; Valeev, E. F.; Sherrill, C. D. *J. Am. Chem. Soc*. **2002**, *124*, 10887.

(40) Sinnokrot, M. O.; Sherrill, C. D. *J. Phys. Chem. A* **2004**, *108*, 10200.

(41) Sinnokrot, M. O.; Sherrill, C. D. *J. Phys. Chem. A* **2006**, *110*, 10656.

(42) Arnstein, S.; Sherrill, C. D. *Phys. Chem. Chem. Phys.* **2008**, *10*, 2646.

(43) Sherrill, C. D.; Takatani, T.; Hohenstein, E. *J. Phys. Chem. A* **2009**, *113*, 10146.

(44) Vasquez-Mayagoitia, A.; Sherrill, C. D.; Aprà, T.; Sumpter, B. G. *J. Chem. Theory Comput.* **2010**, *6*, 727.

(45) Meijer, E. J.; Sprik, M. *J. Chem. Phys.* **1996**, *105*, 8684.

(46) Tsuzuki, S.; Lüthi, H. P. *J. Chem. Phys.* **2001**, *114*, 3949.

(47) Zhao, Y.; Truhlar, D. *J. Chem. Theory Comput.* **2007**, *3*, 289.

(48) Zhao, Y.; Truhlar, D. *J. Chem. Phys.* **2006**, *125*, 194101.

(49) Zhao, Y.; Truhlar, D. *Theor. Chim. Accounts* **2008**, *120*, 215.

(50) Honenstein, E.; Chill, S.; Sherrill, C. *J. Chem. Theory Comput.* **2008**, *4*, 1996.

(51) Grimme, S. *J. Comput. Chem.* **2004**, *25*, 1463.

(52) Grimme, S. *J. Comput. Chem.* **2006**, *27*, 1787.

(53) Hasselmann, A.; Jansen, G. *J. Chem. Phys.* **2005**, *122*, 014103.

(54) Podeszwa, R.; Bukowski, R.; Szalewicz, K. *J. Phys. Chem. A* **2006**, *110*, 10345.

(55) Jaffe, R. L.; Smith, G. D. *J. Chem. Phys.* **1996**, *105*, 2780.

(56) Hobza, P.; Selzle, H. L.; Schlag, E. W. *J. Phys. Chem.* **1996**, *100*, 18790.

(57) Pitoňák, M.; Neogrády, P.; Černý, J.; Grimme, S.; Hobza, P. *ChemPhysChem* **2009**, *10*, 282.

(58) Grimme, S. *J. Chem. Phys.* **2003**, *118*, 9095.

(59) Pitoňák, M.; Hesselmann, A. *J. Chem. Theory Comput.* **2010**, *6*, 168.

(60) Špóner, J.; Leszczynski, J.; Hobza, P. *J. Phys. Chem.* **1996**, *100*, 5590.

(61) Riley, K.; Hobza, P. *J. Phys. Chem. A* **2007**, *111*, 8257.

(62) Rutledge, L.; Durst, H.; Wetmore, S. *J. Chem. Theory Comput.* **2009**, *5*, 1400.

(63) Bizzarri, M.; Cacelli, I.; Prampolini, G.; Tani, A. *J. Phys. Chem. A* **2004**, *108*, 10336.

(64) Boys, S. F.; Bernardi, F. *Mol. Phys.* **1970**, *19*, 553.

(65) Fuhrmann, J.; Rurainski, A.; Lenhof, H.-P.; Neumann, D. *J. Comput. Chem.* **2009**, *30*, 1371.

(66) Frisch, M. J., Trucks, G. W.; Schlegel, H. B.; Scuseria, G. E.; Robb, M. A.; Cheeseman, J. R.; Montgomery, J. A., Jr.; Vreven, T.; Kudin, K. N.; Burant, J. C.; Millam, J. M.; Iyengar, S. S.; Tomasi, J.; Barone, V.; Mennucci, B.; Cossi, M.; Scalmani, G.; Rega, N.; Petersson, G. A.; Nakatsuji, H.; Hada, M.; Ehara, M.; Toyota, K.; Fukuda, R.; Hasegawa, J.; Ishida, M.; Nakajima, T.; Honda, Y.; Kitao, O.; Nakai, H.; Klene, M.; Li, X.; Knox, J. E.; Hratchian, H. P.; Cross, J. B.; Bakken, V.; Adamo, C.; Jaramillo, J.; Gomperts, R.; Stratmann, R. E.; Yazyev, O.; Austin, A. J.; Cammi, R.; Pomelli, C.; Ochterski, J. W.; Ayala, P. Y.; Morokuma, K.; Voth, G. A.; Salvador, P.; Dannenberg, J. J.; Zakrzewski, V. G.; Dapprich, S.; Daniels, A. D.; Strain, M. C.; Farkas, O.; Malick, D. K.; Rabuck, A. D.; Raghavachari, K.; Foresman, J. B.; Ortiz, J. V.; Cui, Q.; Baboul, A. G.; Clifford, S.; Cioslowski, J.; Stefanov, B. B.; Liu, G.; Liashenko, A.; Piskorz, P.; Komaromi, I.; Martin, R. L.; Fox, D. J.; Keith, T.; Al-Laham, M. A.; Peng, C. Y.; Nanayakkara, A.; Challacombe, M.; Gill, P. M. W.; Johnson, B.; Chen, W.; Wong, M. W.; Gonzalez, C.; Pople, J. A. *Gaussian 03*, Revision C.02; Gaussian, Inc.: Wallingford, CT, 2004.

(67) Cacelli, I.; Lami, C.; Prampolini, G. *J. Comput. Chem.* **2009**, *30*, 366.

(68) Cacelli, I.; Prampolini, G.; Tani, A. *J. Phys. Chem. B* **2005**, *109*, 3531.

(69) Cacelli, I.; De Gaetani, L.; Prampolini, G.; Tani, A. *J. Phys. Chem. B* **2007**, *111*, 2130.

CT100172W